



Original Article

Investigation of ^{180}W separation by transient single withdrawal cascade using Salp Swarm optimization algorithm

Morteza Imani, Mahdi Aghaie*

Engineering Department, Shahid Beheshti University, G.C., P.O. Box: 1983963113, Tehran, Iran



ARTICLE INFO

Article history:

Received 14 June 2022

Received in revised form

6 December 2022

Accepted 6 December 2022

Available online 12 December 2022

Keywords:

Single withdrawal cascades

 ^{180}W isotope

Transient condition

Simulation

 q iteration method

Salp Swarm optimization algorithm

ABSTRACT

The ^{180}W is the lightest isotope of Tungsten with small abundance ratio. It is slightly radioactive (α decay), with an extremely long half-life. Its separation is possible by non-conventional single withdrawal cascades. The ^{180}W is used in radioisotopes production and study of metals through gamma-ray spectroscopy. In this paper, single withdrawal cascade model is developed to evaluate multicomponent separation in non-conventional transient cascades, and available experimental results are used for validation. Numerical studies for separation of ^{180}W in a transient single withdrawal cascade are performed. Parameters affecting the separation and equilibrium time of cascade such as number of stages, cascade arrangements, feed location and flow rate for a fixed number of gas centrifuges (GC) are investigated. The Salp Swarm Algorithm (SSA) as a bio-inspired optimization algorithm is applied as a novel method to minimize the feed consumption to obtain desired concentration in the collection tank. Examining different cascade arrangements, it is observed in arrangements with more stages, the separation is further efficient. Based on the obtained results, with increasing feed flow rate, for fixed product concentration, the cascade equilibrium time decreases. Also, it is shown while the feed location is the farthest stage from the collection tank, the separation and cascade equilibrium time are well-organized. Finally, using SSA optimal parameters of the cascade is calculated, and optimal arrangement to produce 5 gr of ^{180}W with 90% concentration in the tank, is proposed.

© 2022 Korean Nuclear Society, Published by Elsevier Korea LLC. This is an open access article under the CC BY license (<http://creativecommons.org/licenses/by/4.0/>).

1. Introduction

Recently, there has been a considerable growth in application of stable isotopes. The stable isotopes have been widely used in many areas such as physics, medicine, bioscience, nuclear, material and environmental sciences [1]. Tungsten is a rare metal found naturally on Earth, usually combined with elements in chemical compounds. Natural Tungsten contains five stable isotopes which are ^{180}W , ^{182}W , ^{183}W , ^{184}W and ^{186}W . The ^{180}W is the lightest and used in the production of ^{181}W radionuclide. It can be used in life science for healthcare, medical applications, pharmaceuticals industries and geophysical studies [2]. The natural abundance of ^{180}W is very low, equals to 0.12%.

GC can be used to separate isotopes with small abundance ratio. In case of ^{180}W , the separation by conventional GC methods is very expensive and takes place in several stages due to the small abundance ratio of ^{180}W .

In 2014, Cheltsov et al. separated Sulphur isotopes by the conventional cascades. The ^{36}S is separated to a concentration of 99% with the four stages [3]. Due to the disadvantages of conventional cascades in the separation of low concentration isotopes, non-conventional transient cascade was invented. Transient cascades were first used by Russian researchers in 1999 to separate the Tellurium isotope up to 99% [4]. Transient cascades are divided into two main categories: Single withdrawal (SW) and No Feed Single Withdrawal (NFSW) cascades [5]. The SW and NFSW cascades are mainly used for the separation of light-heavy, and intermediate isotopes, respectively.

[6] compared the conventional and transient cascades in the separation of the ^{124}Xe . Their results showed the superiority of transient cascades in the separation of light isotope, ^{124}Xe . [7] solved the SW cascade equations using the Crank–Nicolson method and compared the simulation results with the experimental results of a four-stage SW cascade. The results of their simulations were consistent with the experimental results.

Meta-heuristic algorithms are beneficial methods for solving complex problems. Recently, implementation of meta-heuristic

* Corresponding author.

E-mail address: m_ghaie@sbu.ac.ir (M. Aghaie).

Nomenclature

C	Concentration
C'	Product concentration
C''	Waste concentration
H	Holdup
H'	Holdup of upstream pipes
H''	Holdup of downstream pipes
F	External feed flow of each stage
P	External product flow of each stage
W	External waste flow of each stage
L	Feed flow
L'	Product flow
L''	Waste flow
M	Molecular weight
N	Number of stages

Greek characters

θ	Cut
α	Unit separation factor

Subscripts and superscripts

i	Isotope number
a	Parameter after pipes
n	Stage number
m	Number of time step

optimization methods in separation cascades is taken into consideration due to the large number of variables [8–10]. For instance, Mansourzadeh et al. (2018) used the teaching learning-based optimization algorithm with a novel mutation, for tapered and square cascades; and Safdari et al., (2017) applied the particle swarm optimization technique for a counter-current cascade.

In this paper, attempts have been made to study the separation parameters of ^{180}W , in a time dependent SW cascade. For this evaluation, it is necessary to perform the cascade simulation in the transient. In this simulation, due to the greater equilibrium time of concentration, the concentration equations were solved in the transient and in order to simulate SW cascade, the concentration distribution equations have been linearized by q iteration method. To validate numerical calculation of single withdrawal cascade simulation code (SWCS), the experimental results of a SW cascade with 4-stages for separation of SF_6 isotopes performed by the [7]; are used. Using the SWCS code, the square SW cascades with fixed number of GCs and different arrangements are studied to separate the ^{180}W to a concentration of 90%. In a nearly optimum arrangement where this concentration with low equilibrium time is obtained, the effect of feed flow rate and feed location are investigated. In this paper, the Salp Swarm Algorithm (SSA) is introduced as a novel optimization approach for minimizing feed consumption in the SW cascades. For this purpose, using SSA the feed consumption has been minimized to obtain 5 gr of ^{180}W in the collection tank, and the comparison of the results has been done for arrangements.

2. Numerical modelling of cascade

2.1. Single Withdrawal (SW) cascade

In SW cascade, depending on the purpose of separating, a withdrawal will be disconnected. As it depicted in Fig. 1, in type A, due to the recirculation of tail flow of cascade, heavy isotopes are

collected in the left-side tank. In type B, light isotopes are collected in the right-side tank due to the recirculation of the cascade head flow and the position of the tank is in product side.

In the SW cascade simulation, the steady state flow is assumed and transient simulation of concentration distribution is performed; this assumption is due to the short equilibrium time of flows against the concentrations in the cascade [4,11]. In this simulation, the concentration of isotopes in the head and tail flows at each stage is calculated over the time.

2.2. Calculation of interstage flows

The cascade concentration distribution is determined only when the hydraulic conditions of the cascade are known [12]. Due to the steady state flow in the cascade, the hydraulic conditions are independent of time. External hydraulic parameters consist of external feed and withdrawals in stages F_n, W_n, P_n . Internal hydraulic parameters are head and tail flows of the stages L'_n and L''_n , respectively (see Fig. 2).

It is possible to calculate the internal hydraulic parameters using the interstage cuts (θ_n) in mass conservation equations of stages [7].

$$\theta_n = \frac{(L'_n + P_n)}{(L''_n + W_n + L'_n + P_n)} \tag{1}$$

$$0 = L''_n + W_n + L'_n + P_n - F_n - L'_{n-1} - L''_{n+1} \tag{2}$$

The recycling flow ratio in the first stage for type A of SW cascades and in the last stage for type B defines as below:

$$\begin{aligned} \theta_{rec} &= \frac{L'_N}{(L'_N + P_N)} \quad \text{Type A} \\ \theta_{rec} &= \frac{L''_1}{(L''_1 + W_1)} \quad \text{Type B} \end{aligned} \tag{3}$$

The tapered arrangement of GCs in SW cascades can be achieved by adjusting the θ_{rec} . By assuming the steady state flow in the cascade, the head and tail flow of stage will be the same ($L'_n = L''_n$ and $L''_n = L'_n$). Also, the cascade cut will be one and zero in the type A and B SW cascades, respectively.

2.3. Concentration distribution simulation in cascade

Considering a stage in the cascade according to Fig. 2, the mass conservation of i th component is written as Equation (4).

$$\begin{aligned} \frac{\partial H_n \widehat{C}_{i,n}}{\partial t} &= L''_{n+1} C'_{i,n+1} + L'_{n-1} C'_{i,n-1} + F_n C^F_{i,n} - (L''_n + W_n) C''_{i,n} \\ &\quad - (L'_n + P_n) C'_{i,n} \end{aligned} \tag{4}$$

Similarly, for the upstream and downstream pipes, the mass conservation of the i th component written as follows [6].

$$\frac{\partial H'_n \widehat{C}'_{i,n}}{\partial t} = L'_n C'_{i,n} - L''_n C''_{i,n} \tag{5}$$

$$\frac{\partial H''_n \widehat{C}''_{i,n}}{\partial t} = L''_n C''_{i,n} - L'_n C'_{i,n} \tag{6}$$

In Equations 4–6, superscript a represents the parameter after passing through the pipe connecting to stage n . $C'_{i,n}$ and $C''_{i,n}$ are the concentrations of i th component in the head and tail flows, respectively. H is gas inventory, $\widehat{C}_{i,n}$ is average concentration of

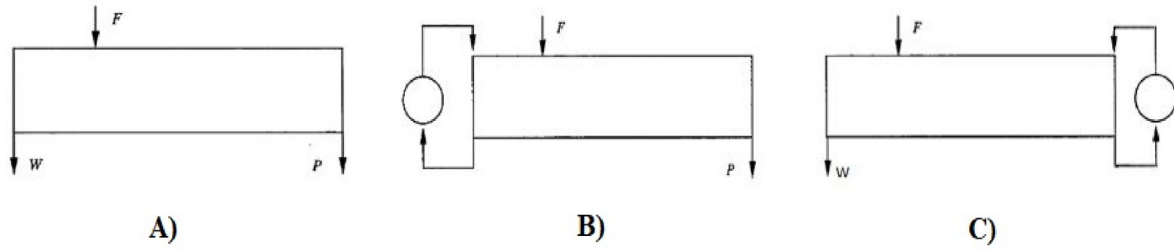


Figure 1. Schematic comparison of A) conventional Square cascade, B) SW cascade type A and C) SW cascade type B

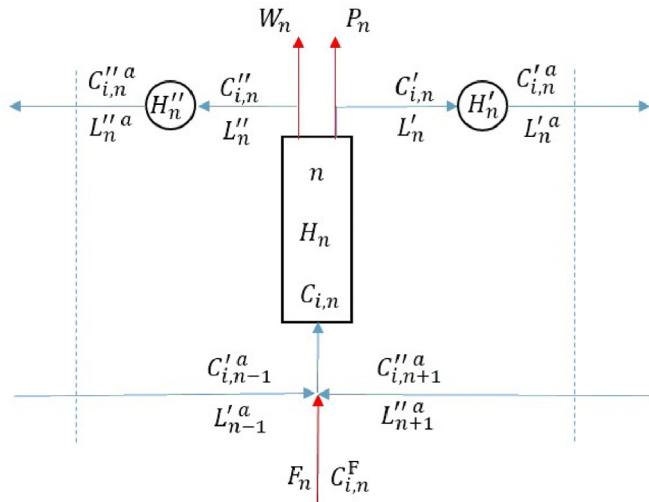


Figure 2. Schematic view from one step of the cascade

isotope *i*th in the stage, $\hat{C}_{i,n}^{\prime}$ denotes average holdup concentration of upstream pipes and $\hat{C}_{i,n}^{\prime\prime}$ stands for the average holdup concentration of the downstream pipes of the stage. The average concentration in the stage (stage inventory concentration, $\hat{C}_{i,n}$) is estimated as the average concentration of stage output flows [13,14].

$$\hat{C}_{i,n} \cong \frac{(L_n'' + W_n)C_{i,n}'' + (L_n' + P_n)C_{i,n}'}{(L_n'' + W_n + L_n' + P_n)} \quad (7)$$

It should be noted that the average concentration of up and downstream pipes is considered as an approximation of the output concentration of the pipes, which is a strict approximation and gives more confidence for the calculations [13].

$$\hat{C}_{i,n}^{\prime} \cong C_{i,n}^{\prime a} \quad (8)$$

$$\hat{C}_{i,n}^{\prime\prime} \cong C_{i,n}^{\prime\prime a} \quad (9)$$

Another used equation is the stage separation factor equation, which is as follows:

$$\frac{C_{i,n}' / C_{i,n}''}{C_{j,n}' / C_{j,n}''} = \alpha_0^{M_j - M_i} \quad (10)$$

With M_i and M_j being the molar weights of the *i*th and *j*th

components, respectively. In addition to the mentioned above equations, the following conditions for the concentration of input and output flows calculations must be set in each stage.

$$\sum_i C_{i,n}' = 1 \quad \sum_i C_{i,n}'' = 1 \quad \sum_i C_{i,n} = 1 \quad (11)$$

To solve Equation (4), the Laasonen implicit finite difference method is used, and after some simplification the below equation obtained.

$$\begin{aligned} -L_{n-1}'^a C_{i,n-1}'^{a(m+1)} + \left(\frac{H_n}{\Delta t} \frac{L_n' + P_n}{(L_n'' + W_n + L_n' + P_n)} + L_n' + P_n \right) C_{i,n}'^{a(m+1)} \\ + \left(\frac{H_n}{\Delta t} \frac{L_n'' + W_n}{(L_n'' + W_n + L_n' + P_n)} + L_n'' + W_n \right) C_{i,n}''^{a(m+1)} \\ - L_{n+1}''^a C_{i,n+1}''^{a(m+1)} = \left(\frac{H_n}{\Delta t} \frac{L_n' + P_n}{(L_n'' + W_n + L_n' + P_n)} \right) C_{i,n}'^{a(m)} \\ + \left(\frac{H_n}{\Delta t} \frac{L_n'' + W_n}{(L_n'' + W_n + L_n' + P_n)} \right) C_{i,n}''^{a(m)} + F_c C_{i,n}^F \end{aligned} \quad (12)$$

In the above equation, the uppercase *m* represents the time step. In Equation (12), the known values which are the concentrations in the previous time interval, are placed on the right side of the equation (*m*), and the values of the unknown concentrations for the current time interval are located on the left side of the equation (*m* + 1). Similarly, by applying the Laasonen method to Equations (5) and (6), these equations will be derived as follows.

$$\left(\frac{H_n'}{\Delta t} + L_n'^a \right) C_{i,n}'^{a(m+1)} - L_n' C_{i,n}'^{a(m)} = \left(\frac{H_n'}{\Delta t} \right) C_{i,n}'^{a(m)} \quad (13)$$

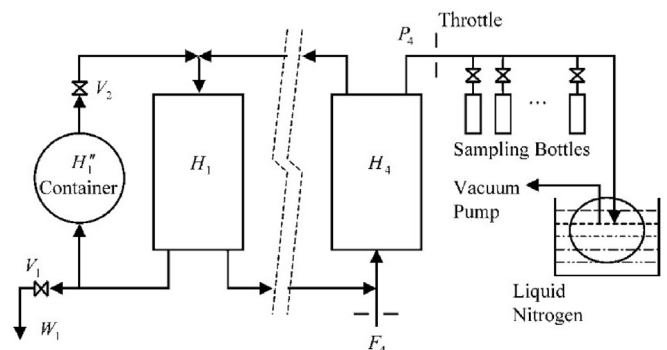


Fig. 3. The SW cascade set up by [7].

Table 1
Natural concentrations of Sulphur isotopes.

Components	³² S	³³ S	³⁴ S	³⁶ S
Concentration	0.95007	0.0076	0.0422	0.00013

Table 2
Cascade specifications used experimentally by Ref. [7] (dimensionless).

Parameter	α_0	$L_{n-0.1.2.3.4}$	P_4	F_4	$H_{n-2.3.4}$	H_1	H'_1
Value	1.5	1	1	1	0.01	0.02	0.09

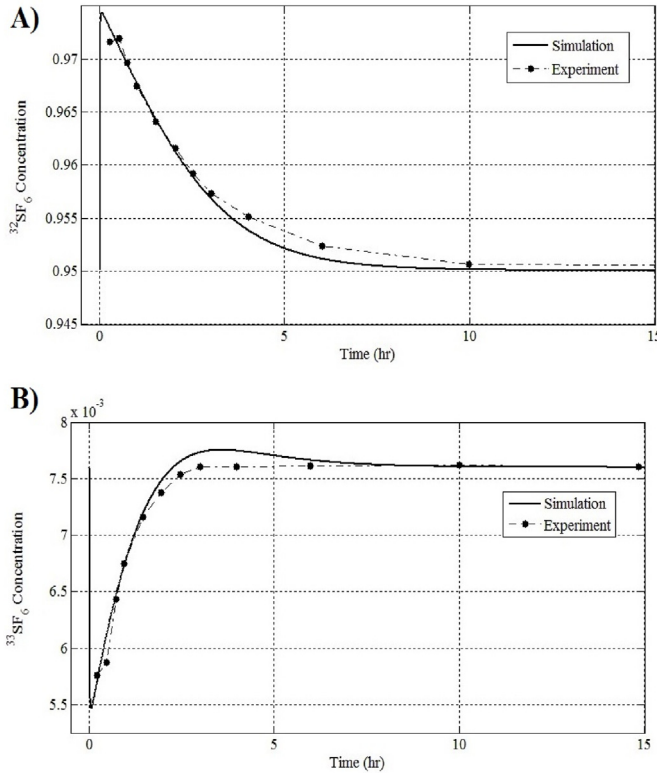


Fig. 4. Comparison of experimental results of [7] with simulation results A) ³²S and B) ³³S concentrations.

$$\left(\frac{H''_n}{\Delta t} + L''_n a\right) C''_{i,n}{}^{a(m+1)} - L''_n C''_{i,n}{}^{(m+1)} = \left(\frac{H''_n}{\Delta t}\right) C''_{i,n}{}^{a(m)} \quad (14)$$

Using Equations (14) and (15), $C''_{i,n}{}^{a(m+1)}$ and $C''_{i,n}{}^{a(m+1)}$ values can be placed in Equation (12), and the obtained equation can be written in the simplified form as below:

$$-\phi_{i,n-1} C'_{i,n-1} + \omega_{i,n} C'_{i,n} + \delta_{i,n} C''_{i,n} - \gamma_{i,n+1} C''_{i,n+1} = r_{i,n} \quad (15)$$

To solve the above equation in each time interval, the q iteration method must be used, and details of this method explained in (Zeng and Ying, 2000b).

Table 3
Natural concentrations of Tungsten isotopes.

Components	¹⁸⁰ W	¹⁸² W	¹⁸³ W	¹⁸⁴ W	¹⁸⁶ W
Concentration	0.0012	0.2650	0.1431	0.3064	0.2843

2.4. Optimization procedure

2.4.1. Fitness function

In this work, the number of GCs has been considered to be fixed, and optimization of effective parameters has been investigated. In SW cascade design, there are four types of parameters which can be optimized including feed location, feed flow rate, the recycle flow ratio and cut of the stages. The holdup of stages and pipes can be defining as a function of flow rates. The objective function specified in this article is as follows:

$$\text{Fitness Function} = 20000 \times (C_{\text{tank}} - C_{\text{desired}})_{+\text{Feed consumption}} \quad (16)$$

$$\text{Feed consumption} = \text{Feed} \times T_{\text{Equilibrium}}$$

Minimizing this fitness value, the feed consumption of cascade will be minimized while the concentration of tank approaches to the desired value. The amount of feed consumption can be obtained by product of the feed flow rate and equilibrium time of concentration.

2.4.2. Salp Swarm Algorithm

Salp Swarm Algorithm (SSA) is a recent bio-inspired optimization method, simulated by foraging and navigation behaviour of salp chain, generally live in deep oceans. In the mathematical model of this algorithm, salp population is divided into two groups called leader and followers. The best salp (best solution) is considered as the food source to be followed by the salp chain. In any iteration, the leader salp changes its position with respect to the food sources. The leader explores and exploits the search space around the best solution and the follower salps move gradually towards the leader. This process helps salps in converging to the global optima and preventing from being trapped in local one. All the details about this algorithm can be found in (Mirjalili et al., 2017).

2.5. Validation of the SWCS code

To check the accuracy of the code, the reported experimental data [7] are used. Fig. 3 shows a schematic of this cascade (SW type A cascade with four stages).

In experimental evaluation of [7]; the process gas was Sulphur hexafluoride. Its natural content is reported in Table 1. Due to the fact that the cascade was a SW type A, heavy isotopes were collected in the tank. Table 2 gives the cascade specifications.

In this cascade, the feed is entered from stage four and the cascade withdrawal is in same stage (see Fig. 3). Fig. 4 shows the concentration of the two Sulphur isotopes at withdrawal of the cascade in term of time.

As shown in Fig. 4A, at the beginning of the separation process, the concentration of the ³²S at the cascade withdrawal increases rapidly and then decreases. Concentration decreasing continue

Table 4
GC specifications and cascade parameters.

Parameter	Value
Cascade feed flow rate	50 gr/hr
Output flow of cascade	50 gr/hr
Feed location stage	1
Cascade cut	0
Total Number of GCs	120
H'_1 (Holdup of collection tank)	1 gr
Optimum feed for GCs	50 gr/hr

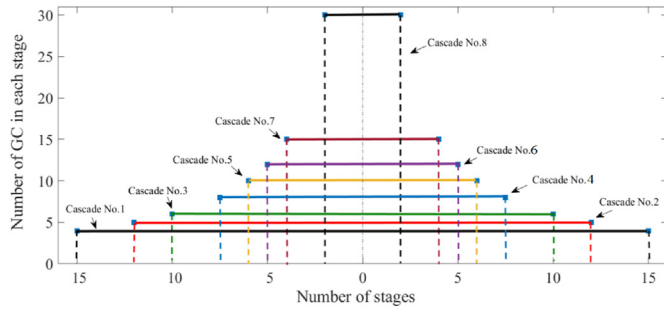


Fig. 5. Different arrangements for square cascades with 120 centrifuges.

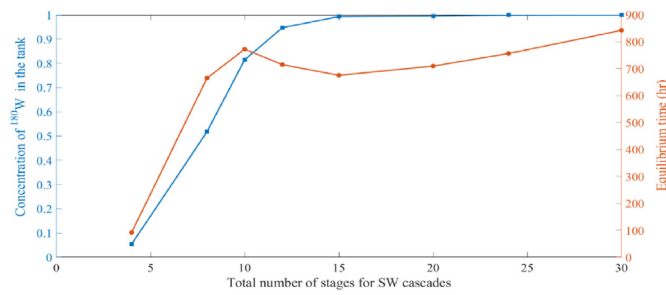


Fig. 6. ¹⁸⁰W concentration in the tank and equilibrium time for all cascades configurations in steady state.

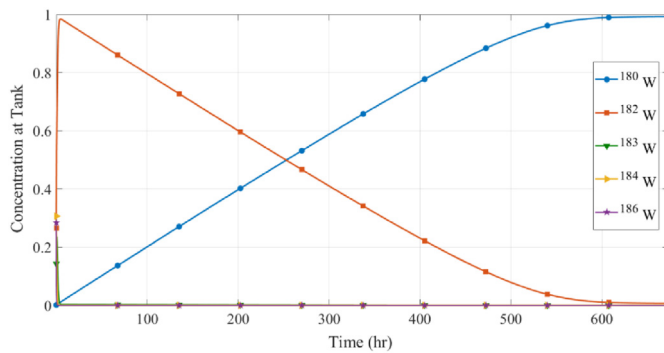


Fig. 7. Concentration of Tungsten isotopes in the tank with time for cascade No. 4.

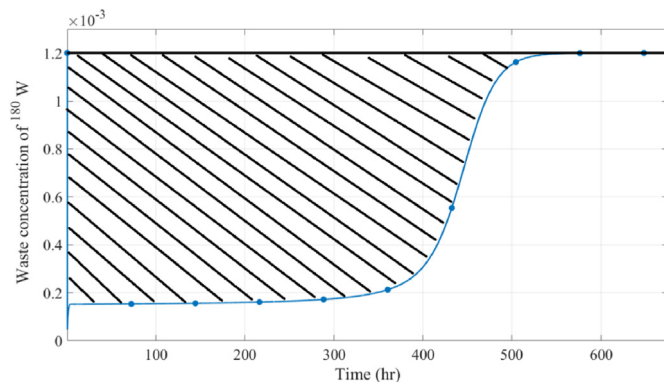


Fig. 8. Concentration of ¹⁸⁰W isotope in the waste side of cascade No. 4.

until steady state condition is reached. In steady state, the cascade withdrawal concentration will be equal to the feed flow concentration. As it can be seen, the results obtained by simulation are

consistent with experimental results reported by Ref. [7].

3. Simulation and results for ¹⁸⁰W separation

To separate the ¹⁸⁰W by square SW cascade, for a given number of GCs, different arrangements must be studied. Table 3 shows the natural concentrations for Tungsten isotopes. In this analysis, the main aim is to separate the ¹⁸⁰W to a concentration over 90% while the number of GCs is considered to be 120. This section contains parametric study of the cascades and optimization of ¹⁸⁰W separation.

3.1. Selection of square SW cascade arrangement for separation of ¹⁸⁰W

In this paper, the number of centrifuges is constant (120). So, different arrangements can be figured; and the most efficient cascade, produces the desired concentration can be selected. In this study, the collection tank is located in the light side (SW cascade type B). That's because the desired isotope (¹⁸⁰W) is the lightest and the light isotope has a higher concentration on the right side of the cascade. So, in order to accumulate the desired isotope, the collection tank would be on the right side just like the SW cascade type B. The feed location and required specifications for parametric study are presented in Table 4. The unit separation factor, holdup of pipes, and GCs are considered as Eq. (17). These equations generated based on the assumption that the unit separation factor is a function of cut and feed flow rate like the relation presented in (Borisevich et al., 2014), and the holdup is a linear function of feed flow rate (Manson, Benedict et al., 1981). The f_{pipe} is pipe flow rate, and f_{GC} is the feed flow rate of a single GC. The holdup of a stage is calculated by multiplying the number of GCs in a holdup.

$$\alpha_0 = (0.7 - 0.5\theta + 0.246\theta^2)(f_{GC})^{-0.08}$$

$$H_{pipe} = 0.00005 * f_{pipe} + 0.005$$

$$H_{GC} = 0.0008 * f_{GC} + 0.01 \tag{17}$$

Fig. 5 shows eight different arrangements of the square cascades with 120 GCs. This figure, shows the number of GCs in each stage for these cascades. The performance of these cascades should be evaluated for ¹⁸⁰W separation.

Performing simulation for steady state, ¹⁸⁰W concentration in tank for proposed arrangements is calculated (see Fig. 6). It can be seen, the cascades No. 1, 2, 3, 4 and 5 have concentration above 90%. In the selected arrangements, the No. 1 has the highest number of stages and No. 5 has the highest (L/F) ratio. Based on Fig. 6, increasing the number of stages has a great effect on the concentration. By increasing the number of stages, the number of

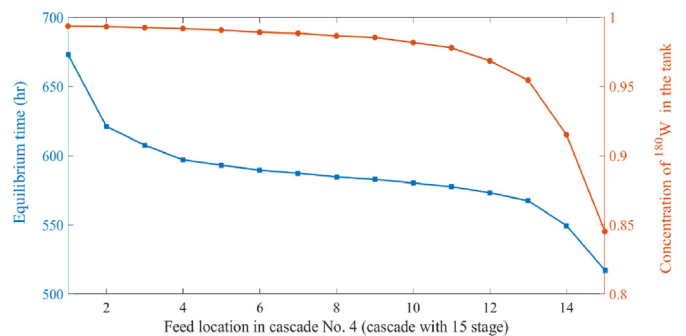


Fig. 9. Equilibrium time and concentration of ¹⁸⁰W in the tank for different feed stages in cascade No. 4.

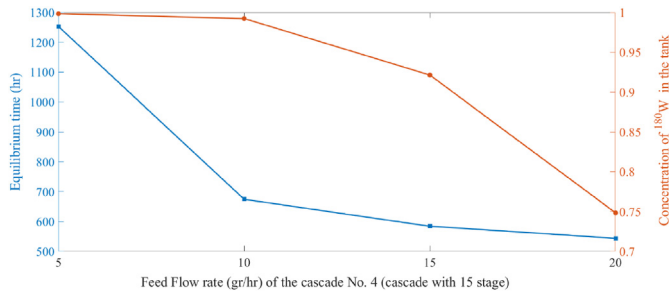


Fig. 10. Equilibrium time and ¹⁸⁰W concentration in the tank for different feed flow rates in cascade No. 4.

enriching stages would increase. So, the trend of this figure is the reverse of Fig. 5. Fig. 6 also shows the equilibrium time for concentration for all cascades. The reason for such a high equilibrium time for these cascades is due to the small abundance ratio of the desired isotope and low feed flow rate. In this case, only 0.06 gr/hr (0.0012*50 gr/hr) of the desired isotope would be entered into the cascade, and only a small amount of this value would be accumulated in the collection tank for each time. By increasing the number of stages, the equilibrium time increases. It is clear that it takes more time for isotopes to reach the ends of longer cascades. It is clear that No. 4 has less equilibrium time for ¹⁸⁰W enrichment, therefore, it is selected for de tail study.

3.2. Concentration distribution in the selected arrangement (No. 4)

The transient concentration of Tungsten isotopes in tank for cascade arrangement No. 4 (SW type B), is shown in Fig. 7. In this cascade, lighter isotopes are moved to the tank over time and the concentration of heavy isotopes will be decreased. By accumulating the ¹⁸⁰W isotopes in tank over time, the ¹⁸⁰W concentration increases at first and when equilibrium is reached, the increase in concentration of the isotope will be stopped. So, the tank can be separated from the cascade.

Fig. 8 displays the concentration of the ¹⁸⁰W in the heavy side of the cascade. The concentration decreases in the initial moments of separation, and increases over time and finally it will be equal the

Table 5

The SSA results for square arrangement of GCs in ¹⁸⁰W separation.

Parameter	Run number							
	1	2	3	4	5	6	7	8
Feed (gr/hr)	10	10	10	10	10	10	10	10
$\theta_{recycle}$	0.138	0.135	0.403	0.134	0.593	0.131	0.526	0.453
θ_1	0.437	0.435	0.455	0.446	0.363	0.42	0.358	0.368
θ_2	0.546	0.579	0.445	0.524	0.483	0.58	0.475	0.552
θ_3	0.405	0.371	0.329	0.405	0.388	0.384	0.406	0.4
θ_3	0.45	0.489	0.53	0.436	0.457	0.526	0.412	0.504
θ_4	0.304	0.288	0.416	0.259	0.401	0.259	0.509	0.455
θ_5	0.327	0.298	0.411	0.326	0.326	0.338	0.337	0.384
θ_6	0.458	0.446	0.321	0.5	0.373	0.526	0.3	0.389
θ_7	0.324	0.315	0.3	0.338	0.311	0.308	0.471	0.381
θ_8	0.387	0.417	0.471	0.387	0.412	0.371	0.323	0.444
θ_9	0.411	0.435	0.391	0.426	0.371	0.455	0.354	0.361
θ_{10}	0.389	0.4	0.365	0.398	0.424	0.384	0.515	0.402
θ_{11}	0.401	0.401	0.4	0.424	0.409	0.41	0.404	0.428
θ_{12}	0.345	0.352	0.344	0.311	0.379	0.356	0.371	0.354
θ_{13}	0.301	0.299	0.3	0.271	0.404	0.353	0.491	0.493
θ_{14}	0.485	0.464	0.484	0.519	0.3	0.404	0.3	0.3
θ_{15}	0.437	0.494	0.455	0.446	0.363	0.42	0.358	0.368
T_{eq} (hr)	489	490	490	493	493	497	502	506
C_{tank}	0.900	0.900	0.899	0.903	0.899	0.905	0.899	0.899
$Feed_{con}$ (gr)	4893	4901	4903	4931	4932	4972	5025	5067

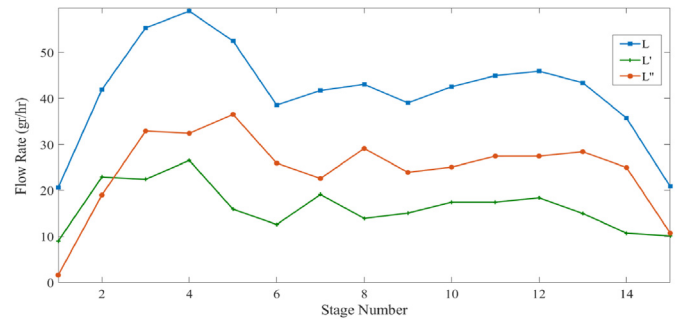


Fig. 11. Flow distribution in the optimal cascade (L, L', L'' are feed, head and tail flow rates, respectively).

Table 6

The concentration of Tungsten in waste flow and tank.

Isotopes	Concentration			
	Feed (t = 0)	Waste (t = 489 h)	Ave. waste con.	Tank (t = 489 h)
¹⁸⁰ W	0.001200	0.00117	0.00018	0.90001
¹⁸² W	0.265000	0.26503	0.26514	0.07610
¹⁸³ W	0.143100	0.14310	0.14325	0.01259
¹⁸⁴ W	0.306400	0.30640	0.30676	0.00987
¹⁸⁶ W	0.284300	0.28430	0.28466	0.00143

feed concentration. The hatched area is equal to the amount of mass accumulation in the tank, stages, and pipes.

3.3. Effect of feed location

To investigate the effect of feed location on the target isotope concentration and cascade equilibrium time for cascade number 4, all parameters are considered constant and the feed location is changed. As shown in Fig. 9, when the feed location is selected in the first stage (NF = 1), the concentration of target isotope in the tank is higher, and the cascade equilibrium time is increased as well. It is due to the fact that the number of enriching stages devoted to the enriching section is maximum and equilibrium times are at the peaks when the feed location is in the first stages. When feed enters to square cascades, interstage flows are different, before and after the feed entrance [13]. Before feed entrance, the interstage cuts are equal. However, after feed entrance, interstage flows are not equal, and the amounts of interstage cuts are different accordingly. So, when feed location is at the first stage, interstage cuts and flows are different at mixing points, which leads to a higher amount of time for reaching equilibrium. Conversely, when the feed location is at the end, all the interstage flows are equal, and it takes lower time to reach equilibrium. As a result, there is 18% and 29% differences in terms of target isotope concentration and cascade equilibrium time between the cascades with feeds of stages 1 and 15, respectively.

3.4. Effect of feed flow rate

To investigate the effect of feed flow rate, the rate in cascade number 4 is changed. The (L/F) ratio of the cascade is also varied to keep the number of GCs and the cascade arrangement constant. Fig. 10 presents the cascade equilibrium time by feed flow rate. It can be clearly seen that by increasing the feed flow, the cascade equilibrium time decreases. When the feed flow is increased from 5 gr/hr to 20 gr/hr, the cascade equilibrium time decreased by 57%. The reason for such behaviour was predictable. The tank with an increase in inlet flow reaches equilibrium sooner. The variation of the target isotope concentration in the tank with different feed flow

Table 7
The SSA results for taper arrangement of GCs in ¹⁸⁰W separation.

parameter	Run number							
	1	2	3	4	5	6	7	8
NF	14	14	14	14	14	14	14	14
Feed (gr/hr)	10	10	10	10	10	10	10	10
$\theta_{recycle}$	0.00	0.00	0.00	0.00	0.00	0.00	0.00	0.00
θ_1	0.399	0.403	0.431	0.301	0.405	0.301	0.300	0.300
θ_2	0.370	0.365	0.373	0.366	0.365	0.346	0.344	0.300
θ_3	0.317	0.317	0.316	0.302	0.317	0.316	0.300	0.300
θ_4	0.387	0.381	0.380	0.456	0.381	0.457	0.300	0.300
θ_5	0.361	0.351	0.348	0.317	0.351	0.313	0.300	0.300
θ_6	0.380	0.375	0.378	0.442	0.374	0.435	0.448	0.310
θ_7	0.368	0.388	0.385	0.309	0.369	0.309	0.480	0.300
θ_8	0.426	0.415	0.416	0.463	0.418	0.472	0.323	0.314
θ_9	0.338	0.356	0.349	0.357	0.360	0.369	0.477	0.300
θ_{10}	0.442	0.442	0.443	0.431	0.442	0.433	0.332	0.416
θ_{11}	0.396	0.398	0.398	0.395	0.397	0.392	0.488	0.528
θ_{12}	0.430	0.428	0.429	0.473	0.429	0.459	0.406	0.465
θ_{13}	0.411	0.409	0.410	0.362	0.411	0.362	0.434	0.567
θ_{14}	0.528	0.525	0.525	0.509	0.525	0.505	0.480	0.600
θ_{15}	0.522	0.554	0.573	0.540	0.555	0.519	0.535	0.419
T_{eq} (hr)	529	531	531	532	532	530	553	554
C_{tank}	0.900	0.899	0.899	0.899	0.899	0.899	0.899	0.899
Feed _{consumption} (gr)	5289	5314	5315	5320	5326	5365	5535	5541

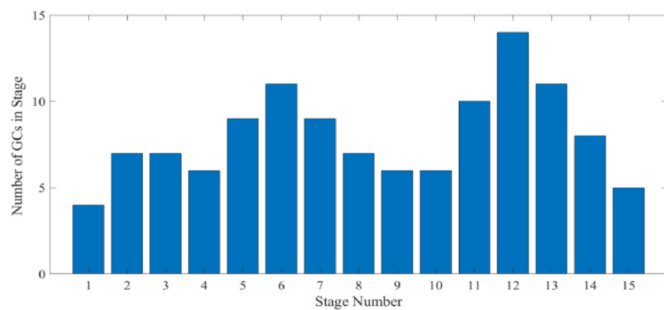


Fig. 12. The arrangement of GCs in the optimum taper cascade.

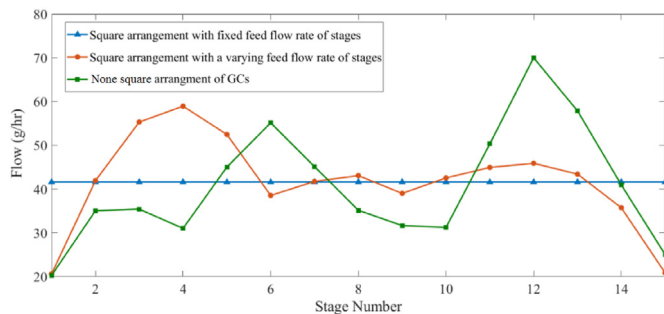


Fig. 13. The comparison of the interstage flow of different obtained SW cascades.

Table 8
Feed consumption for different arrangement of SW cascades.

Cascade arrangement	C_{tank}	T_{eq} (hr)	Feed _{con} (gr)
Square with fixed feed flow rate of stages	0.882	486	4862
Square with varying feed flow rate of stages	0.900	489	4893
Taper cascade	0.900	505	5054

is also shown in Fig. 10. Accordingly, as the feed flow increases with proper (L/F) ratio, due to separation factor level, the target isotope concentration decreases.

3.5. The result of optimization for the selected arrangement

Next to parametric study of the selected arrangement, in order to obtain 5 gr of ¹⁸⁰W of 90% concentration in the collection tank, the optimal parameters are obtained by SSA. It is clear that the number of the variables is large and meta heuristic algorithms are beneficial. The unit separation factor, holdup in pipes and GCs are considered as Eq. (17). The minimum allowable feed flow rate to the GC is 2 gr/hr and the maximum is 20 gr/hr. In this optimization, parameters presented in vector V are optimized using SSA algorithm. After 400 iterations with 20 search agents, all the SSA parameters for the 8 best runs and the lowest fitness values are given in Table 5.

$$V = (Feed, \theta_{recycle}, \theta_1, \theta_2, \theta_3, \theta_4, \theta_5, \theta_6, \theta_7, \theta_8, \theta_9, \theta_{10}, \theta_{11}, \theta_{12}, \theta_{13}, \theta_{14}, \theta_{15}) \tag{18}$$

For the best run (Run No.1), the selected arrangement of GCs produces 5 gr of ¹⁸⁰W with 90% concentration by consuming 4893 gr of natural Tungsten in 489 h, and interstage flow rates of this cascade are presented in Fig. 11. As can be seen, the interstage flow at the beginning and at the end of the cascade reduces. For comparison, the calculation has been done for a conventional square cascade with the same GCs and configuration. Based on the method presented by (Imani et al., 2021b), a conventional square cascade which is optimized by the SSA method, consumes 5124 gr to produce the product. This is about 5% lower than the optimum SW cascade.

The main point that can be concluded from the optimization results is that, in an SW cascade, it is more optimal that the interstage flows at the beginning and end of the cascade be fewer than the intermediate stages.

In Table 6, the concentration of isotopes is presented in waste side and in tank. As can be seen, the concentrations of isotopes in waste at the equilibrium time are almost equal to the concentrations of isotopes in the feed flow. The third column shows the average concentrations of isotopes in waste flow over time.

It is clear the presented arrangement has square shape but internal feed flows of the stages are not equal, along the cascade. In this section another test case is added for more justifications. In order to obtain an optimum arrangement of 120 GCs for a SW cascade, the optimization is carried out with varying GCs number in each stage (15 stages). The whole procedure is same as last case with a little difference in fitness function. The total number of GCs is added to the fitness function as a constraint.

$$Fitness\ Func = 20000 * (C_{tank} - C_{desired})_+ + Feed\ consumption + |total\ No.\ GCs - 120| \tag{19}$$

In each iteration, after calculating interstage flows, the number of GCs in each stage can be obtained by dividing the feed flow rate of the stage by the feed flow of a GC. The feed flow of a GC can be considered to the optimum feed flow where the separation power of the GC is maximum. To compare the optimal taper cascade with the optimal square cascade introduced in last section, two cascades must have equal total interstage flow. So, the feed flow of a GC in taper considered as Eq. (20).

$$\frac{total\ interstage\ flow\ of\ the\ optimal\ square\ cascade}{total\ number\ of\ GCs} = 5.2\ g/hr \tag{20}$$

After 400 iterations with 20 search agents, all the SSA parameters for the 8 best runs and the lowest fitness values are given in

Table 7.

For the best run (Run No.1), the selected arrangement of GCs produces 5 gr of ^{180}W with 90% concentration by consuming 5289 gr of natural Tungsten in 529 h. In Fig. 12, as can be seen, the arrangement of GCs in the optimum cascade is not as conventional square cascades.

Fig. 13 shows the comparison of interstage flows of the introduced cascades in previous sections. All of these cascades have the same total feed flow rate and total number of GCs. This figure also shows internal feed flow rate for the adopted conventional square cascade. This cascade is total mass flow adaption of the optimum cascade with variable flow rates.

In Table 8, the amount of feed consumption for producing 5 gr of ^{180}W with 90% in the tank is presented. It shows that the square cascade with fixed feed flow rate of GCs in each stage cannot produce the desired concentration in the tank, and between the second and third cases, the square arrangement with a varying feed flow rate of GC consumes fewer natural feed of Tungsten.

4. Conclusion

In this study, to enrich the ^{180}W to a concentration of 90%, the different arrangements of the SW transient cascade were studied by numerical simulation. It was observed that for a certain number of centrifuges, increasing the number of steps is preferable, and the longer a cascade is, the higher concentration and equilibrium time can be obtained. By examining the effect of feed location, it was observed that moving away the feed location from the tank, increases the concentration and equilibrium time. Investigating the feed flow rate effect, it was indicated that with an increase in feed flow rate, the cascade equilibrium time and the desired isotope concentration in tank decreases. By selecting the 15-stage cascade with 8 GCs in each stage (cascade No. 4), the SSA optimization algorithm is used to minimize the feed consumption for obtaining 5 gr of ^{180}W isotope in the tank with 90% concentration. The optimum square cascade with a varying feed flow rate of GCs produced this amount of product after 489 h and consuming 4893 gr of natural Tungsten. In the next case, the SSA optimization for a taper arrangement obtained a different arrangement that consumes 3% more amount of natural feed for the same amount of product. Also, it is shown that conventional square cascade with the same total flow rate could not reach to desired concentration.

Declaration of competing interest

The authors declare that they have no known competing financial interests or personal relationships that could have appeared to influence the work reported in this paper.

References

- [1] A. Mundl, R.J. Walker, J.R. Reimink, R.L. Rudnick, R.M. Gaschnig, Tungsten-182 in the upper continental crust: evidence from glacial diamictites, *Chem. Geol.* 494 (2018) 144–152, <https://doi.org/10.1016/j.chemgeo.2018.07.036>.
- [2] A.A. Orlov, A.A. Ushakov, V.P. Sovach, R.V. Malyugin, Mathematical modeling of nonstationary separation processes in a cascade of gas centrifuges for separation of tungsten isotopes, *J. Eng. Phys. Thermophys.* 91 (2018) 565–573, <https://doi.org/10.1007/s10891-018-1777-0>.
- [3] A.N. Cheltsov, N.S. Babaev, L.Y. Sosnin, Y.D. Shipilov, A.V. Bespalov, P.V. Mochalov, V.K. Khamylov, Centrifugal enrichment of sulfur isotopes, *J. Radioanal. Nucl. Chem.* 299 (2014) 989–993.
- [4] Y. Cao, S. Zeng, Z. Lei, C. Ying, Study of a nonstationary separation method with gas centrifuge cascade, *Separ. Sci. Technol.* 39 (2004) 3405–3429, <https://doi.org/10.1081/SS-200034331>.
- [5] M. Imani, A.R. Keshkar, A. Rashidi, J.K. Sabet, A. Noroozi, Investigation on the effect of holdup and cascade shape in NFSW cascades, *Prog. Nucl. Energy* 119 (2020), 103182, <https://doi.org/10.1016/j.pnucene.2019.103182>.
- [6] S. Zeng, C. Ying, Separating isotope components of small abundance, *Separ. Sci. Technol.* 37 (2002) 3577–3598, <https://doi.org/10.1081/SS-120014445>.
- [7] S. Zeng, M. Zhou, C. Ying, Theoretical and experimental study of a non-stationary isotope separation process in a gas centrifuge cascade, *Separ. Sci. Technol.* 38 (2003) 2375–2394, <https://doi.org/10.1081/SS-120022278>.
- [8] F. Ezazi, M. Imani, J. Safdari, M. Mallah, S.L. Mirmohammadi, An application of nature-inspired paradigms in the overall optimization of square and squared-off cascades to separate a middle isotope of tellurium, *Ann. Nucl. Energy* 171 (2022), 109033, <https://doi.org/10.1016/j.anucene.2022.109033>.
- [9] M. Imani, M. Aghaie, M. Adelikhah, Introducing optimum parameters of separation cascades for ^{123}Te using GWO based on ANN, *Ann. Nucl. Energy* 163 (2021), 108545, <https://doi.org/10.1016/j.anucene.2021.108545>.
- [10] S. Khooshechin, F. Mansourzadeh, M. Imani, J. Safdari, M.H. Mallah, Optimization of flexible square cascade for high separation of stable isotopes using enhanced PSO algorithm, *Prog. Nucl. Energy* 140 (2021), 103922, <https://doi.org/10.1016/j.pnucene.2021.103922>.
- [11] A.Y. Smirnov, G.A. Sulaberidze, V.D. Borisevich, S. Zeng, D. Jiang, Transient processes in Q-cascades for separation of multicomponent mixtures, *Chem. Eng. Sci.* 127 (2015) 418–424, <https://doi.org/10.1016/j.ces.2014.12.063>.
- [12] M. Imani, M. Aghaie, A. Keshkar, Numerical simulation of hydrodynamic performance of taper cascades in transient conditions, *Ann. Nucl. Energy* 176 (2022), 109287, <https://doi.org/10.1016/j.anucene.2022.109287>.
- [13] S. Zeng, C. Ying, Transient process in gas centrifuge cascades for separation of multicomponent isotope mixtures, *Separ. Sci. Technol.* 36 (2001) 3439–3457, <https://doi.org/10.1081/SS-100107913>.
- [14] S. Zeng, C. Ying, A robust and efficient calculation procedure for determining concentration distribution of multicomponent mixtures, *Separ. Sci. Technol.* 35 (2000) 613–622, <https://doi.org/10.1081/SS-100100179>.